

# Long-term two-photon neuroimaging with a photostable AIE luminogen

Jun Qian,<sup>1</sup> Zhenfeng Zhu,<sup>1</sup> Chris Wai Tung Leung,<sup>2</sup> Wang Xi,<sup>3</sup> Liling Su,<sup>4</sup> Guangdi Chen,<sup>4</sup> Anjun Qin,<sup>5</sup> Ben Zhong Tang<sup>2,5,\*</sup> and Sailing He<sup>1,\*</sup>

<sup>1</sup>State Key Laboratory of Modern Optical Instrumentations, Centre for Optical and Electromagnetic Research, Zhejiang Provincial Key Laboratory for Sensing Technologies; JORCEP (Sino-Swedish Joint Research Center of Photonics), Zhejiang University, 310058 Hangzhou, China

<sup>2</sup>Department of Chemistry, The Hong Kong University of Science & Technology, Clear Water Bay, Kowloon, Hong Kong, China

<sup>3</sup>Department of Neurobiology, School of Medicine, Zhejiang University, Zijingang Campus, Hangzhou 310058, China

<sup>4</sup>Bioelectromagnetics Laboratory, School of Medicine, Zhejiang University, Hangzhou 310058, China

<sup>5</sup>SCUT-HKUST Joint Research Laboratory, Guangdong Innovative Research Team, State Key Laboratory of Luminescent Materials and Devices, South China University of Technology (SCUT), Guangzhou 510640, China

\*sailing@jorcep.org, tangbenz@ust.hk

**Abstract:** In neuroscience, fluorescence labeled two-photon microscopy is a promising tool to visualize *ex vivo* and *in vivo* tissue morphology, and track dynamic neural activities. Specific and highly photostable fluorescent probes are required in this technology. However, most fluorescent proteins and organic fluorophores suffer from photobleaching, so they are not suitable for long-term imaging and observation. To overcome this problem, we utilize tetraphenylethene-triphenylphosphonium (TPE-TPP), which possesses aggregation-induced emission (AIE) and two-photon fluorescence characteristics, for neuroimaging. The unique AIE feature of TPE-TPP makes its nanoaggregates resistant to photobleaching, which is useful to track neural cells and brain-microglia for a long period of time. Two-photon fluorescence of TPE-TPP facilitates its application in deep *in vivo* neuroimaging, as demonstrated in the present paper.

©2015 Optical Society of America

**OCIS codes:** (160.4890) Organic materials; (160.2540) Fluorescent and luminescent materials; (190.4180) Multiphoton processes; (170.3880) Medical and biological imaging; (180.2520) Fluorescence microscopy; (180.4315) Nonlinear microscopy.

## References and links

1. A. Li, H. Gong, B. Zhang, Q. Wang, C. Yan, J. Wu, Q. Liu, S. Zeng, and Q. Luo, "Micro-optical sectioning tomography to obtain a high-resolution atlas of the mouse brain," *Science* **330**(6009), 1404–1408 (2010).
2. D. A. Boas, T. Gaudette, G. Strangman, X. Cheng, J. J. A. Marota, and J. B. Mandeville, "The accuracy of near infrared spectroscopy and imaging during focal changes in cerebral hemodynamics," *Neuroimage* **13**(1), 76–90 (2001).
3. D. Bastien, A. Gallagher, J. Tremblay, P. Vannasing, M. Thériault, M. Lassonde, and F. Lepore, "Specific functional asymmetries of the human visual cortex revealed by functional near-infrared spectroscopy," *Brain Res.* **1431**, 62–68 (2012).
4. X. Wang, Y. Pang, G. Ku, X. Xie, G. Stoica, and L. V. Wang, "Noninvasive laser-induced photoacoustic tomography for structural and functional *in vivo* imaging of the brain," *Nat. Biotechnol.* **21**(7), 803–806 (2003).
5. X. Yang and L. V. Wang, "Monkey brain cortex imaging by photoacoustic tomography," *J. Biomed. Opt.* **13**(4), 044009 (2008).
6. F. Helmchen, M. S. Fee, D. W. Tank, and W. Denk, "A miniature head-mounted two-photon microscope. High-resolution brain imaging in freely moving animals," *Neuron* **31**(6), 903–912 (2001).
7. Y. X. Wu, X. L. Liu, W. Zhou, X. H. Lv, and S. Q. Zeng, "Observing neuronal activities with random access two-photon microscope," *J. Innov. Opt. Health Sci.* **2**(01), 67–71 (2009).
8. G. S. He, L. S. Tan, Q. Zheng, and P. N. Prasad, "Multiphoton absorbing materials: Molecular designs, characterizations, and applications," *Chem. Rev.* **108**(4), 1245–1330 (2008).
9. D. Kobat, M. E. Durst, N. Nishimura, A. W. Wong, C. B. Schaffer, and C. Xu, "Deep tissue multiphoton microscopy using longer wavelength excitation," *Opt. Express* **17**(16), 13354–13364 (2009).

10. N. G. Horton, K. Wang, D. Kobat, C. G. Clark, F. W. Wise, C. B. Schaffer, and C. Xu, "In vivo three-photon microscopy of subcortical structures within an intact mouse brain," *Nat. Photonics* **7**(3), 205–209 (2013).
11. M. Maletic-Savatic, R. Malinow, and K. Svoboda, "Rapid dendritic morphogenesis in CA1 hippocampal dendrites induced by synaptic activity," *Science* **283**(5409), 1923–1927 (1999).
12. J. White and E. Stelzer, "Photobleaching GFP reveals protein dynamics inside live cells," *Trends Cell Biol.* **9**(2), 61–65 (1999).
13. T. S. Chen, S. Q. Zeng, Q. M. Luo, Z. H. Zhang, and W. Zhou, "High-order photobleaching of green fluorescent protein inside live cells in two-photon excitation microscopy," *Biochem. Biophys. Res. Commun.* **291**(5), 1272–1275 (2002).
14. Y. G. Meng, J. Liang, W. L. Wong, and V. Chisholm, "Green fluorescent protein as a second selectable marker for selection of high producing clones from transfected CHO cells," *Gene* **242**(1-2), 201–207 (2000).
15. J. B. Birks, *Photophysics of Aromatic Molecules* (Wiley, London, 1970).
16. J. Luo, Z. Xie, J. W. Y. Lam, L. Cheng, H. Chen, C. Qiu, H. S. Kwok, X. Zhan, Y. Liu, D. Zhu, and B. Z. Tang, "Aggregation-induced emission of 1-methyl-1,2,3,4,5-pentaphenylsilole," *Chem. Commun. (Camb.)* **18**(18), 1740–1741 (2001).
17. Z. F. Zhu, X. Y. Zhao, W. Qin, G. D. Chen, J. Qian, and Z. P. Xu, "Fluorescent AIE dots encapsulated organically modified silica (ORMOSIL) nanoparticles for two-photon cellular imaging," *Sci. China-Chem.* **56**(9), 1247–1252 (2013).
18. D. Wang, J. Qian, W. Qin, A. Qin, B. Z. Tang, and S. He, "Biocompatible and photostable AIE dots with red emission for in vivo two-photon bioimaging," *Sci Rep* **4**, 4279 (2014).
19. W. Qin, D. Ding, J. Liu, W. Z. Yuan, Y. Hu, B. Liu, and B. Z. Tang, "Biocompatible nanoparticles with aggregation-induced emission characteristics as far-red/near-infrared fluorescent bioprobes for in vitro and in vivo imaging applications," *Adv. Funct. Mater.* **22**(4), 771–779 (2012).
20. H. Cheng, W. Qin, Z. F. Zhu, J. Qian, A. J. Qin, B. Z. Tang, and S. L. He, "Nanoparticles with aggregation-induced emission for monitoring long time cell membrane interactions," *Prog. Electromagnetics Res.* **140**, 313–325 (2013).
21. K. Li, W. Qin, D. Ding, N. Tomczak, J. Geng, R. Liu, J. Liu, X. Zhang, H. Liu, B. Liu, and B. Z. Tang, "Photostable fluorescent organic dots with aggregation-induced emission (AIE dots) for noninvasive long-term cell tracing," *Sci Rep* **3**, 1150 (2013).
22. G. Feng, C. Y. Tay, Q. X. Chui, R. Liu, N. Tomczak, J. Liu, B. Z. Tang, D. T. Leong, and B. Liu, "Ultrabright organic dots with aggregation-induced emission characteristics for cell tracking," *Biomaterials* **35**(30), 8669–8677 (2014).
23. C. W. T. Leung, Y. Hong, S. Chen, E. Zhao, J. W. Y. Lam, and B. Z. Tang, "A photostable AIE luminogen for specific mitochondrial imaging and tracking," *J. Am. Chem. Soc.* **135**(1), 62–65 (2013).
24. J. Qian, D. Wang, F. H. Cai, W. Xi, L. Peng, Z. F. Zhu, H. He, M. L. Hu, and S. He, "Observation of multiphoton-induced fluorescence from graphene oxide nanoparticles and applications in in vivo functional bioimaging," *Angew. Chem. Int. Ed. Engl.* **51**(42), 10570–10575 (2012).
25. G. S. He, T. C. Lin, S. J. Chung, Q. D. Zheng, C. G. Lu, Y. P. Cui, and P. N. Prasad, "Two-, three-, and four-photon-pumped stimulated cavityless lasing properties of ten stilbazolium-dyes solutions," *J. Opt. Soc. Am. B* **22**(10), 2219–2228 (2005).
26. Q. Zheng, H. Zhu, S. C. Chen, C. Tang, E. Ma, and X. Chen, "Frequency-upconverted stimulated emission by simultaneous five-photon absorption," *Nat. Photonics* **7**(3), 234–239 (2013).
27. R. Weissleder and V. Ntziachristos, "Shedding light onto live molecular targets," *Nat. Med.* **9**(1), 123–128 (2003).

## 1. Introduction

During the past few years, neuro/brain-imaging has attracted much research interest, and many optical technologies have been proposed in order to obtain accurate and complete neural information [1–7]. Among them, multiphoton fluorescence microscopy plays a very important role. Relying on the simultaneous absorption of two or more near-infrared photons by a fluorophore [8], multiphoton microscopy is capable of achieving deeper tissue penetration and efficient light detection noninvasively, and is thus very suitable for thick-tissue and *in vivo* bioimaging [9,10].

Suitable fluorescent agents are very important for multiphoton-microscopy-assisted neuro/brain-imaging. In addition to the capability to specifically target neurons, another vital requirement of fluorescent agents is high photostability, which is very helpful in achieving dynamic tracking of neural activities for a long period of time. Fluorescent proteins have been widely applied in neuroscience, since they are biocompatible and have a very high quantum yield [11]. However, they are prone to photobleaching in long-term imaging processes [12,13]. Moreover, the process for transfecting fluorescent protein into experimental animals is time-consuming [14]. Organic fluorophore is another alternative type of fluorescent agent. However, most of them suffer from a severe aggregation-caused quench (ACQ) effect [15],

which means their fluorescence is quenched at high molecule concentrations. To avoid this limitation, very diluted solutions of these fluorophores are used for imaging, and such small numbers of molecules can be easily photobleached under laser beam excitation.

We have discovered a diametrically opposite phenomenon of aggregation-induced emission (AIE) [16]. The propeller-shaped AIE molecules are non-emissive when they are monodispersed in solution, but become highly fluorescent upon the formation of aggregates. Based on this mechanism, hydrophobic AIE molecules can be encapsulated with various types of nanoparticles [17,18], or form nanoaggregates in an aqueous solution spontaneously. All the nanoprobe are very resistant to photobleaching even under high-power laser irradiation [19–21], which is very helpful to long-term dynamic biological imaging and observation [22].

Tetraphenylethene-triphenylphosphonium (TPE-TPP) is an AIE-active luminogen, which has been used for specific mitochondrial imaging and tracking in our previous study [23]. In this paper, we found TPE-TPP can specifically stain primary neurons *in vitro*, as well as brain-microglia *in vivo*. In addition to photobleaching resistance in its nanoaggregates, TPE-TPP also features distinct two-photon fluorescence. Under a 740 nm-femtosecond (fs) laser excitation, it emitted bright cyan fluorescence. We took advantage of these characteristics to perform long-term *in vitro* and *in vivo* neuroimaging.

## 2. Experimental section

### 2.1 Materials

Dimethylsulfoxide (DMSO), N,N-dimethylformamide (DMF) and phosphate buffered saline (PBS, 1X) were obtained from Sinopharm Chemical Reagent Co., Ltd. Poly-L-lysine and Cytosine Arabinoside were purchased from Sigma Aldrich. Cell-culture products, unless otherwise mentioned, were purchased from Invitrogen Gibco. TPE-TPP was synthesized following our previous work [23].

### 2.2 Optical instruments

Absorption and transmission spectra of TPE-TPP were recorded on a Shimadzu 3600 UV-vis scanning spectrophotometer. Photoluminescence spectra of TPE-TPP samples were measured with a HITACHI F-2500 fluorescence spectrophotometer. For the measurement of two-photon fluorescence of TPE-TPP, a Ti-sapphire fs laser (80 MHz, Mira HP, Coherent, Inc.) was used as the excitation source. The fs laser beam was coupled into an objective (10X, NA = 0.25) to achieve high excitation intensity towards the TPE-TPP sample. The excited two-photon fluorescence was collected forward by another objective (10X, NA = 0.25) and recorded with an optical fiber spectrometer (PG 2000, Ideaoptics Instruments), after passing through a short-pass filter.

### 2.3 Culture of primary neurons

All procedures for the isolation of rat neurons were reviewed and approved by the Animal Ethics Committee at Zhejiang University (Approval ID ZJU2009102020). Efforts were made to reduce animal suffering and the number of animals used. Briefly, cerebral cortex neurons in primary culture were prepared from E16-day-old Sprague Dawley rats embryos. Meninges were removed and cortex were cut into pieces and dissociated by trypsin then plated at a density of  $2.5 \times 10^5$  cells/cm<sup>2</sup> in 35 mm Petri dishes previously coated with 100 µg/mL poly-L-lysine in Dulbecco's Modified Eagle Medium (DMEM) supplemented with 10% horse serum. Cells were incubated at 37 °C in a humidified atmosphere containing 5% CO<sub>2</sub> and 95% air. 4 hours after plating, the medium was replaced with Neurobasal Medium supplemented with 2% B27 Supplement, 1% L-glutamine, 100 units/mL penicillin and 100 µg/mL streptomycin. Two days after plating, 2.5 µM Cytosine Arabinoside was added to the culture for 48 hours to inhibit the outgrowth of non-neuronal cells. The medium was renewed every 3 days with 1 mL of warm medium. Neurons were treated with TPE-TPP on day 7.

## 2.4 *In vitro* imaging of primary neurons

Primary neurons were grown on 35 mm cultivation dishes. To confirm the localization of TPE-TPP in primary neurons, 2  $\mu\text{L}$  of a 5 mM stock solution of TPE-TPP in DMSO was added into a 2 mL culture medium for treatment. An upright confocal microscope (Olympus, BX61W1-FV1000) was used for two-photon fluorescence microscopic imaging of primary neurons, and the wavelength of the excitation fs laser was 740 nm. Two-photon fluorescence of TPE-TPP was detected by a PMT (photomultiplier tube), which was equipped with an optical filter to avoid the interference of the excitation source. To study the photostability of TPE-TPP under the two-photon excitation, 50 scans of primary neurons were performed (4.2 s/scan), and the two-photon fluorescence intensity of TPE-TPP in each image was calculated and compared, accordingly.

## 2.5 *In vivo* brain imaging of mice

All the animal experiments were performed in compliance with the Zhejiang University Animal Study Committee's requirements for the care and use of laboratory animals in research. The animal housing area (located in Animal Experimentation Center of Zhejiang University) was maintained at 24 °C with a 12 hour-light/dark cycle, and animals were fed with water and standard laboratory chow. 8-week-aged female BALB/c mice were used for brain imaging. After anesthetized with pentobarbital, the skulls of the mice were opened up through microsurgery. A 0.2  $\mu\text{L}$  stock solution of TPE-TPP in DMSO was microinjected into the brain of mice. The depth of the injected sample was about 300  $\mu\text{m}$ . *In vivo* brain imaging was performed on the same upright confocal microscope (Olympus, BX61W1-FV1000, objective: 25X, NA = 1.05, work distance = 2 mm; wavelength of excitation fs laser: 740 nm). For the description of the immobilization of mice's heads and how the objective of the upright two-photon scanning microscope was arranged to contact the brain, we refer to our previous work [24].

## 3. Results and discussion

### 3.1 Absorption and emission of TPE-TPP

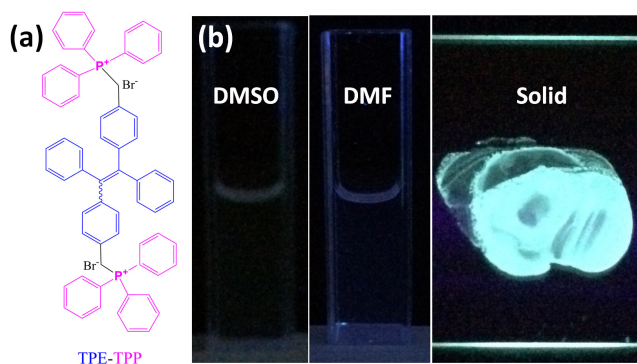


Fig. 1. (a) Chemical structure of TPE-TPP molecule. (b) Photographs of DMSO solution (left), DMF solution (middle) and solid powder (right) of TPE-TPP taken under UV irradiation. Concentration of TPE-TPP: 10  $\mu\text{M}$ .

Figure 1(a) shows the molecular structure of TPE-TPP. A typical AIE luminogen called tetraphenylethene (TPE) is functionalized with two triphenylphosphonium (TPP) groups. TPE-TPP has typical AIE feature. It is almost non-fluorescent in its benign organic solvent, e.g., DMF, DMSO, while it is strongly emissive in the solid state, with a cyan fluorescence (Fig. 1(b)). The absorption spectrum of TPE-TPP is centered at 320 nm (Fig. 2(a)). In aqueous solution containing 0.1% DMSO, TPE-TPP (5  $\mu\text{M}$ , the identical condition for the neuron

staining described below) forms nanoaggregates (Fig. 2(c)), and emits fluorescence centered at a wavelength of 480 nm (Fig. 2(b)).

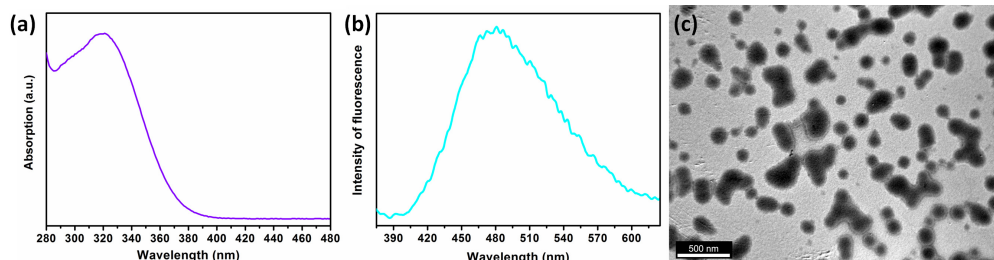


Fig. 2. (a) Absorption spectrum of TPE-TPP. (b) Fluorescence spectrum of TPE-TPP (5  $\mu$ M) nanoaggregates in water, under the excitation of 320 nm. (c) A typical TEM image of TPE-TPP nanoaggregates. Scale bar: 500 nm.

### 3.2 Chemical stability analysis of TPE-TPP nanoaggregates

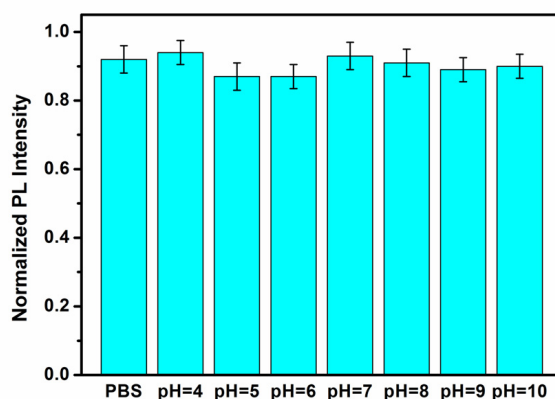


Fig. 3. Fluorescence intensity changes of TPE-TPP (5  $\mu$ M) nanoaggregates treated with PBS, and pH 4 to 10 solutions for 18 h (normalized by the initial fluorescence peak intensity at 0 h). Excitation wavelength: 320 nm.

To confirm the chemical stabilities of TPE-TPP nanoaggregates, we systematically studied the fluorescence intensity changes of these nanoaggregates under different treatments (e.g., PBS, and pH 4 to 10 solutions) for 18 hours. As is known, PBS is a buffer solution commonly used in biological research. pH = 4 and 10 are almost the limit values of pH in the human body. 2  $\mu$ L of a 5 mM stock solution of TPE-TPP in DMSO was added into a 2 mL PBS solution and aqueous solutions with different pH values (e.g., 4 to 10), to form TPE-TPP nanoaggregates in various chemical conditions. The fluorescence intensity of all the samples at 0 hour and 18 hours was measured, accordingly. As shown in Fig. 3, even after 18 hours, the fluorescence peak intensities of TPE-TPP nanoaggregates changed by less than 15% in all experimental conditions (normalized by the initial fluorescence peak intensity at 0 hour), indicating that the TPE-TPP nanoaggregates were chemically stable in those solutions, which is very positive for various bio-applications.

### 3.3 Two-photon fluorescence of TPE-TPP

As is known, multiphoton absorption occurs at a wavelength where there is no or negligible linear absorption [25,26]. Figure 4(a) shows the transmission spectrum of TPE-TPP in the DMSO solution with a path length of 1 cm. It has negligible linear absorption around 740 nm, and this wavelength was chosen for the two-photon excitation of TPE-TPP molecules. Figure 4(b) shows the two-photon fluorescence spectrum of TPE-TPP in solid state, which was excited

by a fs laser at 740 nm. It is centered at 480 nm, and its envelope is very similar to the fluorescence spectrum of TPE-TPP nanoaggregates under one-photon excitation (Fig. 2(b)). As shown in Fig. 4(c), the two-photon induced emission intensity of TPE-TPP is proportional to the square of the fs excitation intensity, confirming the characterization of a two-photon process.

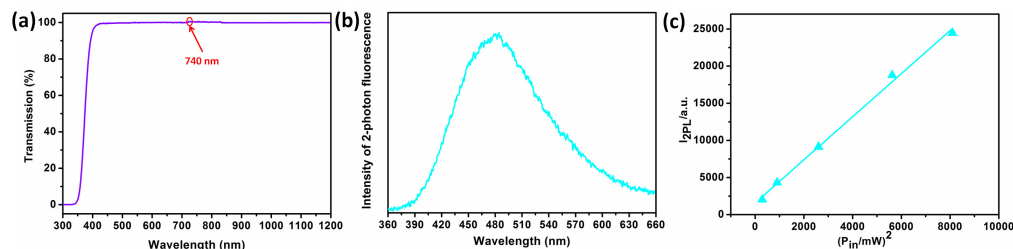


Fig. 4. (a) Transmission spectrum of TPE-TPP in DMSO (1 cm-thickness). (b) Two-photon fluorescence spectrum of TPE-TPP in solid state. (c) Square dependence of two-photon fluorescence of solid TPE-TPP on excitation intensity of the 740 nm-fs laser.

### 3.4 Two-photon fluorescence imaging of primary neurons stained with TPE-TPP

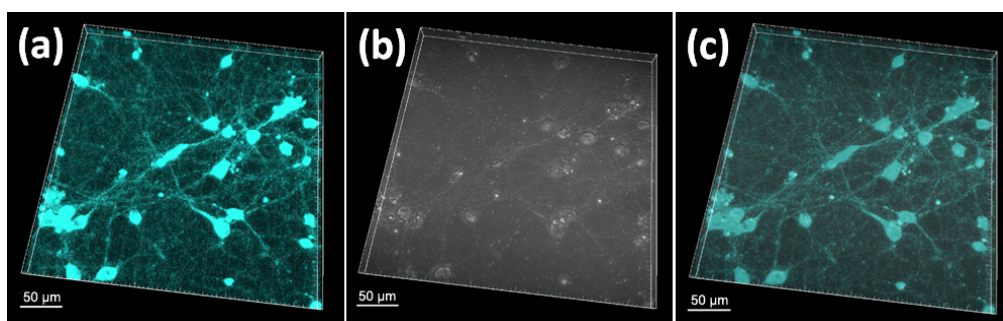


Fig. 5. Two-photon fluorescence images of primary neurons treated with TPE-TPP (5  $\mu$ M) for 2 hours, under the excitation of a fs laser at 740 nm. (a) Fluorescence channel, (b) Bright-field channel, and (c) Merged channel. The scale bar is 50  $\mu$ m.

Primary neurons of mice were treated with 5  $\mu$ M TPE-TPP for 2 hours. After washed with PBS (1X) twice, the cell dish was imaged with a two-photon fluorescence microscope (Olympus, BX61W1-FV1000) under a 740 nm-fs excitation. Figure 5 shows the imaging results. Bright two-photon fluorescence of TPE-TPP was observed from the fluorescence image. The fluorescence signals overlapped very well with the morphologies of neurons (e.g., soma, dendrite and axon) in the bright-field image, indicating that the TPE-TPP nanoaggregates were effectively taken up by neurons. The reason why TPE-TPP can target and light up primary neurons effectively can be explained as follows. TPE-TPP has relatively poor solubility in aqueous solution. When added into aqueous cell culture medium, TPE-TPP molecules formed nanoaggregates (as introduced in Section 3.1). The net positive charges on the nanoaggregates then facilitate them to diffuse across the cell membrane, and then stain the neurons. In addition, due to the AIE feature, TPE-TPP nanoaggregates emitted brighter fluorescence than its single molecule state under two-photon excitation.

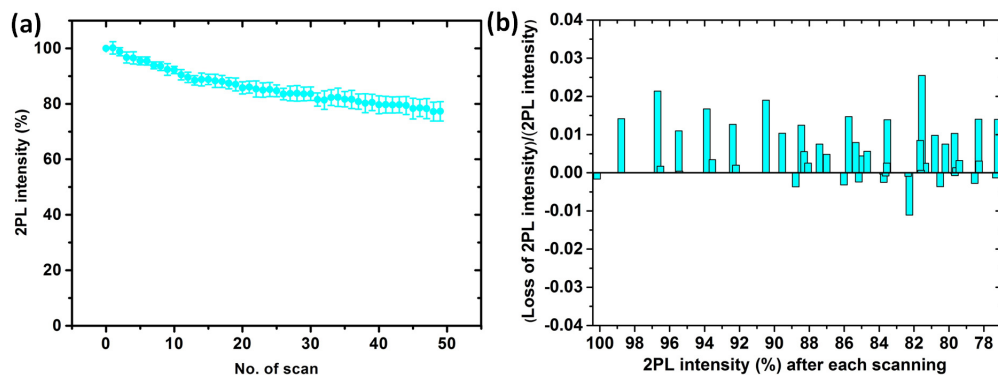


Fig. 6. (a) Two-photon fluorescence intensity (%) of TPE-TPP in neurons with increasing number of scans. Excitation time: 4.2 s/scan; excitation wavelength of the fs laser: 740 nm. (b) Loss ratio of two-photon fluorescence intensity [(two-photon fluorescence intensity before each scan - two-photon fluorescence intensity after each scan)/two-photon fluorescence intensity after each scan] with the two-photon fluorescence intensity (%) after each scan.

Photobleaching resistance is one of the most important advantages of AIE luminogens [19–21], and previously we have proved this feature of TPE-TPP nanoaggregates under one-photon excitation [23]. Herein, we studied the photostability of TPE-TPP under two-photon excitation, by utilizing a 740 nm-fs laser. Primary neurons were stained with 5  $\mu\text{M}$  TPE-TPP for 2 hours. The initial two-photon fluorescence intensity referring to the first scan of TPE-TPP stained cells was used for normalization, and the percentage of signal intensity after each additional scan was calculated. As shown in Fig. 6(a), although the primary neurons have experienced 50 scans (4.2 s/scan), the signal loss of TPE-TPP in the neurons was less than 20%, which means the primary neurons was still “bright” enough to be distinguished after long-term excitation. In addition, the function describing the dependence of “loss ratio of two-photon fluorescence intensity” on the “two-photon fluorescence intensity from the neurons after each scan” was shown in Fig. 6(b). The loss ratios of two-photon fluorescence intensity after all scans were very low (not exceeding 0.03), which means the TPE-TPP nanoaggregates were resistant to photobleaching under 740 nm-fs-excitation. These results illustrated AIE-active TPE-TPP is very suitable for dynamic two-photon imaging and observation of *in vitro* neurons.

### 3.5 Long-term *in vivo* two-photon fluorescence imaging of brain-microglia stained with TPE-TPP

Due to the advantages of deep tissue imaging capability, high spatial resolution, and low thermal damage towards bio-samples, two-photon fluorescence microscopy is a very powerful tool for brain imaging of small animals. We utilized TPE-TPP for the staining of brain-microglia of mice and *in vivo* two-photon fluorescence imaging. After the experimental mice were anesthetized, the skulls of the mice were opened up through microsurgery, and 0.2  $\mu\text{L}$  TPP-TPP in DMSO was microinjected into the brain of mice at a depth of about 300  $\mu\text{m}$ . Figure 7(a) shows the typical three-dimensional (3D) two-photon fluorescence image of the brain of a mouse. The cyan spots, which represent the distribution of TPE-TPP, could be discriminated easily from the background. We also performed one-photon fluorescence imaging of the mouse brain by using a 405 nm-CW excitation, but no fluorescence signal could be observed (data not shown here). This is because violet excitation light has large attenuation (due to water absorption [27] and tissue scattering) in the mouse brain, and its penetrating depth is quite limited, so the TPE-TPP nanoaggregates locating 300  $\mu\text{m}$  below the brain could not be excited. For two-photon microscopy, a 740 nm-fs laser was adopted. Water absorption of light at this wavelength is quite low [27], and 740 nm-light also has lower tissue scattering than 405

nm-light, so the 740 nm-fs laser could penetrate deeper in the mouse brain and effectively excite the two-photon fluorescence of TPE-TPP nanoaggregates.

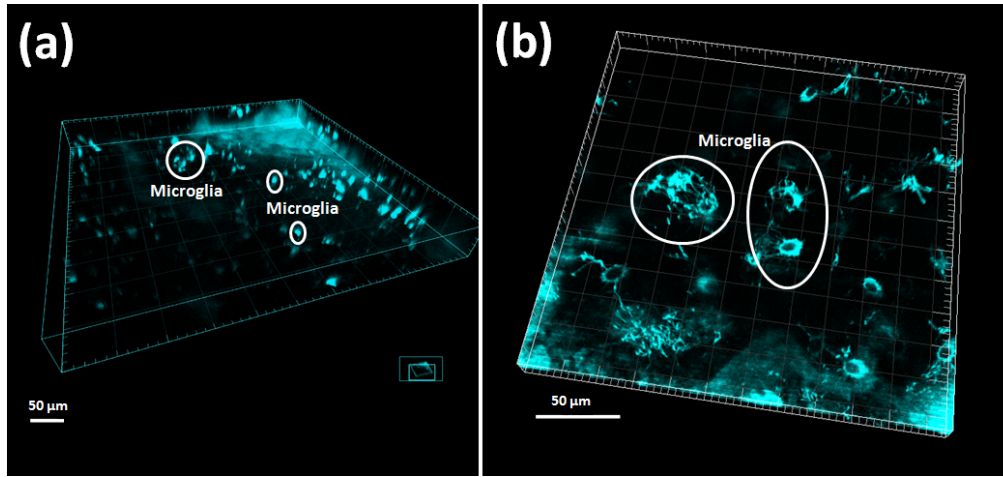


Fig. 7. (a) A reconstructed 3D image illustrating the staining of TPE-TPP in the microglia of a mouse's brain (30 minutes post-treatment) via the two-photon scanning microscope. Scale bar: 50  $\mu\text{m}$ . (b) A magnified 3D two-photon fluorescence image of the brain of a mouse. Scale bar: 50  $\mu\text{m}$ .

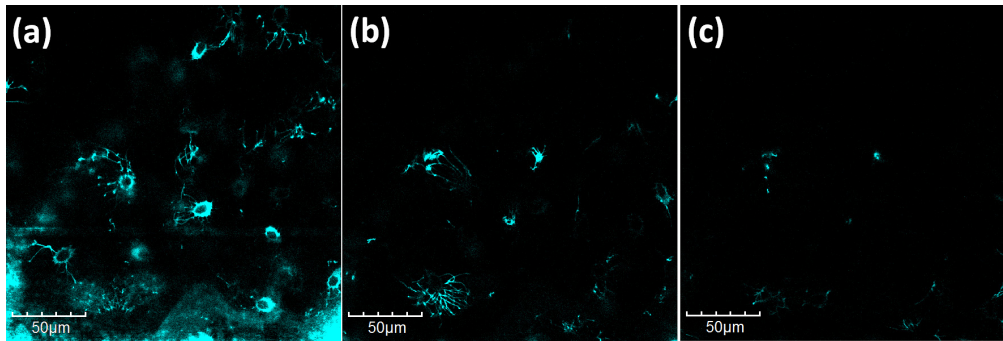


Fig. 8. 2D two-photon fluorescence images at different sections of the *in vivo* mouse brain. (a) The image at the top section. (b) The image at the middle section. (c) The image at the bottom section. Scale bar: 50  $\mu\text{m}$ .

Figure 7(b) is the locally magnified 3D two-photon fluorescence image of the brain of a mouse, and Fig. 8(a)-(c) are the magnified 2D images at different sections of the *in vivo* mouse brain, from which we can obtain more details of imaging. We observed that the brain-microglia was effectively stained by the TPE-TPP nanoaggregates. Due to the bright two-photon fluorescence from TPE-TPP, the morphologies of the microglia could be clearly discriminated. The TPE-TPP nanoaggregates were widely distributed in the somas, dendrites and axons of the microglia, which was similar to the phenomenon in *in vitro* primary neurons. When microinjected into the mouse brain, TPE-TPP molecules formed nanoaggregates in the hydrophilic biological environment, and the net positive charges on TPE-TPP nanoaggregates then facilitated them to stain microglia *in vivo*.

Considering the anti-photobleaching feature of TPE-TPP nanoaggregates under two-photon excitation, we further performed the long-term *in vivo* imaging of mice brains. Vivid 4D (X-Y-Z and time) reconstructed videos are shown in “Media 1” and “Media 2”. With the help of two-photon fluorescence of TPE-TPP, we could observe a slight movement of the microglia, which was accompanied by the breath of the mouse. Figure 9(a) shows the magnified 2D



images of the mouse brain at various points in time. Although the microglia has experienced 81 scans (4.2 s/scan) under the 740 nm-fs laser excitation, the two-photon fluorescence of TPE-TPP staining in the microglia still kept very bright, and negligible signal loss was observed (Fig. 9(b)). The function describing the dependence of “loss ratio of two-photon fluorescence intensity” on the “two-photon fluorescence intensity from the microglia after each scan” was also shown in Fig. 9(c). The loss ratios of two-photon fluorescence intensity after all scans were very low (not exceeding 0.06). Based on two-photon microscopy, photobleaching resistant TPE-TPP nanoaggregates may be applied in various *in vivo* neuroscience studies, e.g., neural stimulation and regulation, or brain-functional behavior recording, which require long-time dynamic observation.

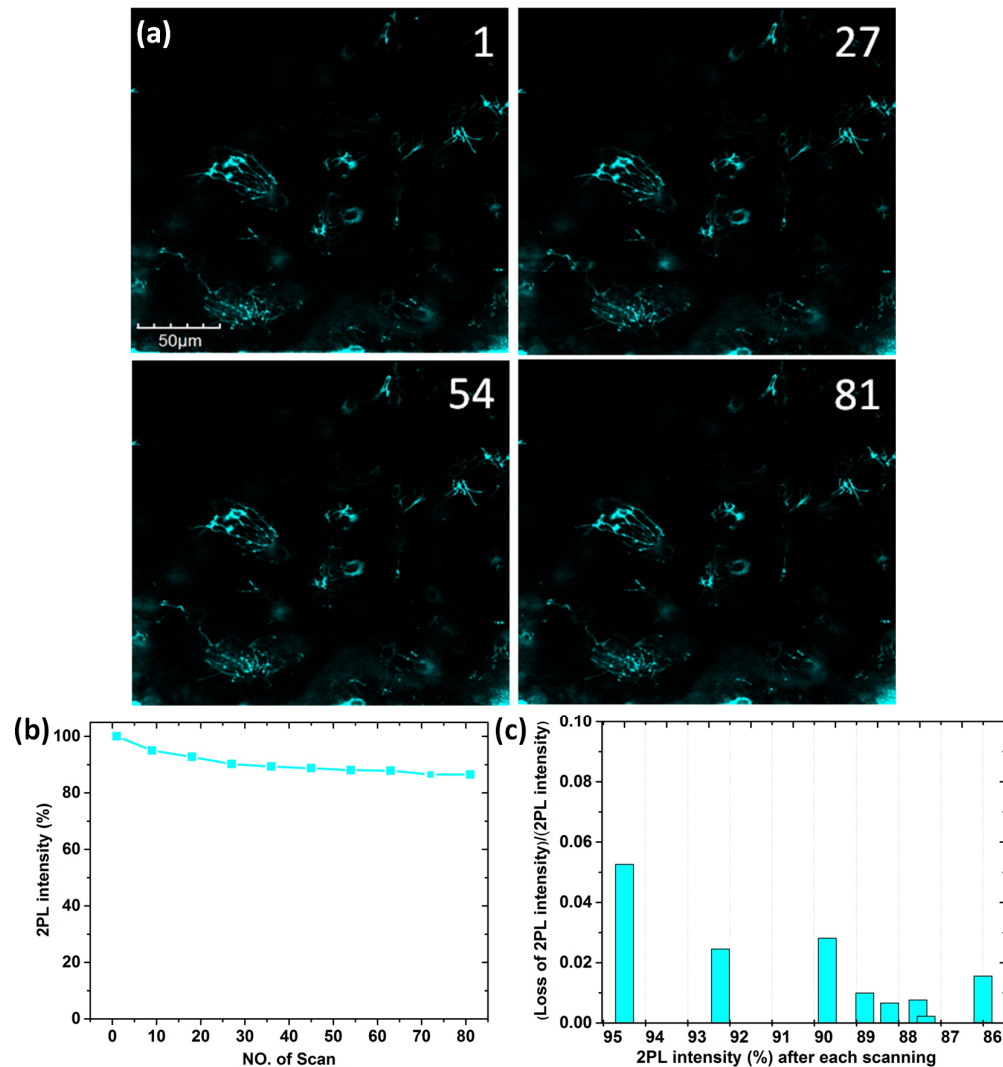


Fig. 9. (a) 2D two-photon fluorescence images of a mouse's brain treated with TPE-TPP, with increasing number of scans (1st, 27th, 54th, and 81st scan; excitation time: 4.2 s/scan). Scale bar: 50 μm (Media 1 and Media 2). (b) Two-photon fluorescence intensity (%) of TPE-TPP in the microglia with increasing scanning time. (c) Loss ratio of two-photon fluorescence intensity [(two-photon fluorescence intensity before each scan - two-photon fluorescence intensity after each scan)/two-photon fluorescence intensity after each scan] with the two-photon fluorescence intensity (%) after each scan.

#### 4. Conclusions

In summary, TPE-TPP, which is an AIE-active luminogen, possesses photobleaching resistance in its nanoaggregates under two-photon excitation. It can also effectively stain the primary neurons in cell dishes, as well as the brain-microglia of mice. Due to its unique features, TPE-TPP can be used for long-term neuroimaging both *in vitro* and *in vivo*. Photostable TPE-TPP may be a good candidate for various *in vivo* neuroscience studies, with the help of two-photon microscopy.

#### Acknowledgments

This work was supported by National Basic Research Program of China (973 Program; 2013CB834704 and 2011CB503700), the National Natural Science Foundation of China (61275190 and 91233208), the Program of Zhejiang Leading Team of Science and Technology Innovation (2010R50007), the Fundamental Research Funds for the Central Universities, the Swedish Research Council, SOARD, and The Research Grants Council of Hong Kong (HKUST2/CRF/10). J.Q. is grateful to Miss S. S. Liu and Miss W. Yin for help in *in vivo* experiment.